

New Hetero Silicon-Carbon Nanostructure Formation Mechanism

S. P. Song,^a M. A. Crimp,^b V. M. Ayres^{a,*}, C. J. Collard,^c J. P. Holloway,^c
and M. L. Brake^c

^a*Department of Electrical and Computer Engineering, Michigan State University,
East Lansing, Michigan, 48824, USA*

^b*Department of Chemical Engineering and Materials Science, Michigan State University,
East Lansing, Michigan, 48824, USA*

^c*Department of Nuclear Engineering and Radiological Sciences, University of Michigan,
Ann Arbor, Michigan, 48109, USA*

We report the formation of silicon and carbon hetero-nanostructures in an inductively coupled plasma system by a simultaneous growth/etching mechanism. Multi-walled carbon nanotubes were grown during one, three and five hour depositions, while tapered silicon nanowires were progressively etched. The carbon and silicon nanostructures and the interfaces between them were studied by electron microscopies and micro Raman spectroscopies. The potential of this method for large-scale controlled production of nano heterostructures without the requirement of a common catalyst is explored.

Keywords: Carbon Nanotubes, Silicon Nanowires, Heterostructure, Inductively Coupled Plasma.

1. INTRODUCTION

Nanoscale heterojunctions between silicon and other nanotube/nanowire materials may have important applications in nanoscale electronic devices, and as interfaces between new nano-materials and conventional silicon electronics. Formation of such nano-heterostructures by means of a common catalyst and a Liquid-Metal-Solid (LMS) growth mechanism for both parts of the heterostructure have been recently reported.^{1, 2, 3, 4} In the present work, we report on an alternative method for the formation of a hetero carbon nanotube-silicon nanowire interface, based on LMS-growth of a carbon nanotube and simultaneous etching of a silicon nanowire.

We have grown carbon nanostructures of approximately micron-scale lengths in an inductively coupled plasma system, using a 20-nanometer layer of iron catalyst on a p-type (100) silicon wafer in methane-hydrogen-argon plasma. The carbon nanostructures were shown to be multi-walled carbon nanotubes and hollow core vapor grown carbon nanofibers. Simultaneously, we have etched tapered silicon nanowires that retain the (100) orientation and crystallinity of the original silicon substrate. Increasing reactor times resulted in a progressive etch of the silicon nanowires. Junctions were observed between the silicon and carbon nanostructures, and details of these are reported.

The simultaneous growth/etching was achieved in an inductively coupled plasma system. Inductively coupled plasmas (ICP) have high radial uniformity and low pressure/low temperature operating characteristics⁵ that make them attractive for large-scale applications. Therefore, the importance of these experiments is that they indicate a mechanism through which large-scale fabrication of integrated nanostructures may be achieved. Also, increased flexibility in material combinations may be achieved, as the common catalyst requirement of References [1–4] is relaxed.

2. EXPERIMENTAL DETAILS

The inductively coupled plasma system was based on a modified Gaseous Electronics Conference (GEC) Reference cell.⁶ The original GEC reactor had two parallel electrodes, 2.54 cm apart. The bottom electrode was biased with a 13.56 MHz radio frequency (RF) power supply at 50 Watts. In the modified cell, the top electrode was replaced by a 5-turn coil that was also powered by a 13.56 MHz RF power supply at 475 Watts. The pressure of the gas mixture was 100 mTorr with 87% Argon, and 6.5% methane and 6.5% hydrogen. Argon was used to sustain the plasma in the inductively coupled mode. Further details are reported in Reference [7].

Samples were prepared by forming a 10–20 nm thick iron layer on a p-type (100) silicon substrate, using laser ablation.⁸ Individual depositions were carried out over

*Author to whom correspondence should be addressed.

time periods of 1 hour 0 minutes, 3 hours 10 minutes and 5 hours 23 minutes. For brevity, the resulting samples will be referred to as the 1-hour, 3-hour and 5-hour samples.

Scanning electron microscopy (SEM), transmission electron microscopy (TEM) with selected area diffraction (SAD), high-resolution transmission electron microscopy (HRTEM) with Energy Dispersive x-ray Spectroscopy (EDS), and micro-Raman Spectroscopy and Surface Enhanced micro Raman Spectroscopy (SERS) were used to characterize the resulting carbon and silicon nanostructures. The SEM was performed using a Cam Scan 44FE. The TEM was performed using a Hitachi H-800 operated at 200 kV and the HRTEM was performed using a JEOL JEM 2010F operated at 200 kV, at Michigan State University. A JEOL 4000 EX operated at 400 kV at the University of Michigan was also used for some of the HRTEM analysis. Samples were prepared for TEM/HRTEM by wetting the surface of the sample with ethanol and gently scraping, followed by dispersing the ethanol and sample via a pipette onto holey carbon film TEM grids.

The micro Raman spectroscope consisted of a 0.75 m double monochromator coupled with an optical microscope, operated in backscattering configuration, with an argon ion laser as the excitation source. 514.5 nm and 488 nm excitation wavelengths were both used in these investigations. SERS spectroscopy was performed as described in Ref. [9], using 20 nm of sputtered gold on a glass substrate.

3. RESULTS AND DISCUSSION

3.1. Scanning Electron Microscopy Results

For the three deposition time periods, SEM images taken at 0° tilt showed a uniform sparse coverage of fibrous nanostructures on a dotted background. A typical example from the five-hour sample is shown in Fig. 1. The coverage appeared to be uniform over roughly 4 cm² sample areas. Upon tilting to 40°, it became apparent that the dotted backgrounds were tips of tapered nanostructures perpendicular to the surface. Interfaces between the fibrous and tapered nanostructures were observed by SEM, as shown in Fig. 1 (a) and (b).

3.2. Transmission Electron Microscopy and Selected Area Diffraction Results and Micro-Raman Results

TEM analysis indicated that the fibrous nanostructures observed in the surface plane had hollow cores and micron-scale lengths, as shown in Fig. 2 (a)–(c). Selected area diffraction (SAD) patterns of these nanostructures revealed spot splitting of about 30°, consistent with that expected for nanotubes.¹⁰ An example of a typical diffraction pattern is shown in Fig. 3. Micro-Raman and SERS spectroscopies of the 5-hour sample also indicated the presence of

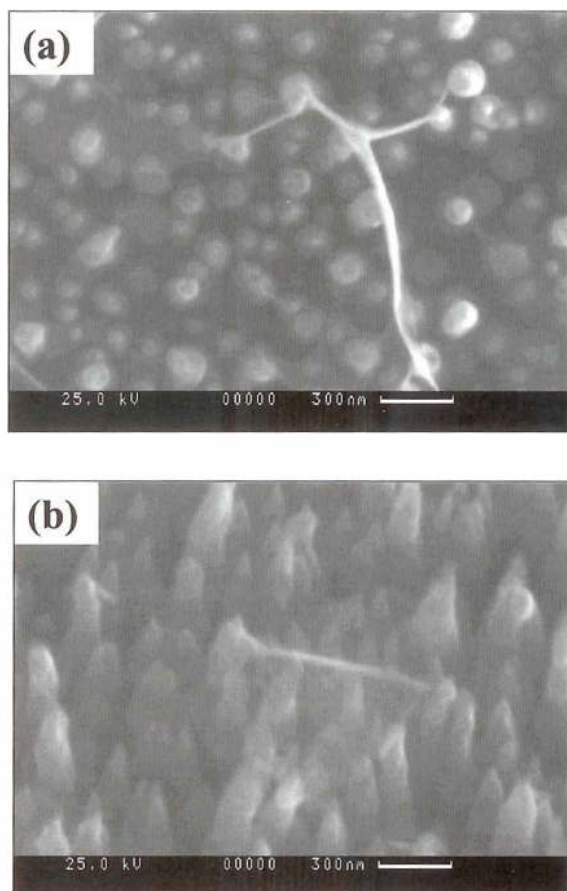


Fig. 1. SEM images taken at (a) top view: 0° tilt and (b) side view: 40° tilt, indicate junctions between the fibrous and the tapered nanostructures.

well-graphitized carbon by relatively sharp peaks at about 1580 cm⁻¹, with 8–10 cm⁻¹ full width half maximum (FWHM). A typical peak is shown in Fig. 4.

TEM analysis of the tapered nanostructures is shown in Fig. 5. The lengths of these nanostructures varied systematically as a function of reactor time. Approximate average lengths of 0.4 microns, 0.5 microns and 0.9 microns were observed for the 1-hour, 3-hour and 5-hour samples. The average base width for the 1-hour and 3-hour samples was about 100 nm, while the average base width for the 5-hour sample was about 150 nm. Typical examples of the progressively etched silicon nanowires are shown in Fig. 6.

Selected area diffraction (SAD), which included tilting to multiple zone axes, showed that these tapered structures were single crystal silicon nanostructures with the [100] orientation along the long axis. The orientation analysis is shown in Fig. 7. The structures were tapered silicon nanowires, not hollow core silicon nanotubes.

TEM images revealed dark contrast dots of about 5–20 nm at the tips or along the sides of most of the tapered silicon nanowires, as shown in Fig. 8. These dark contrast

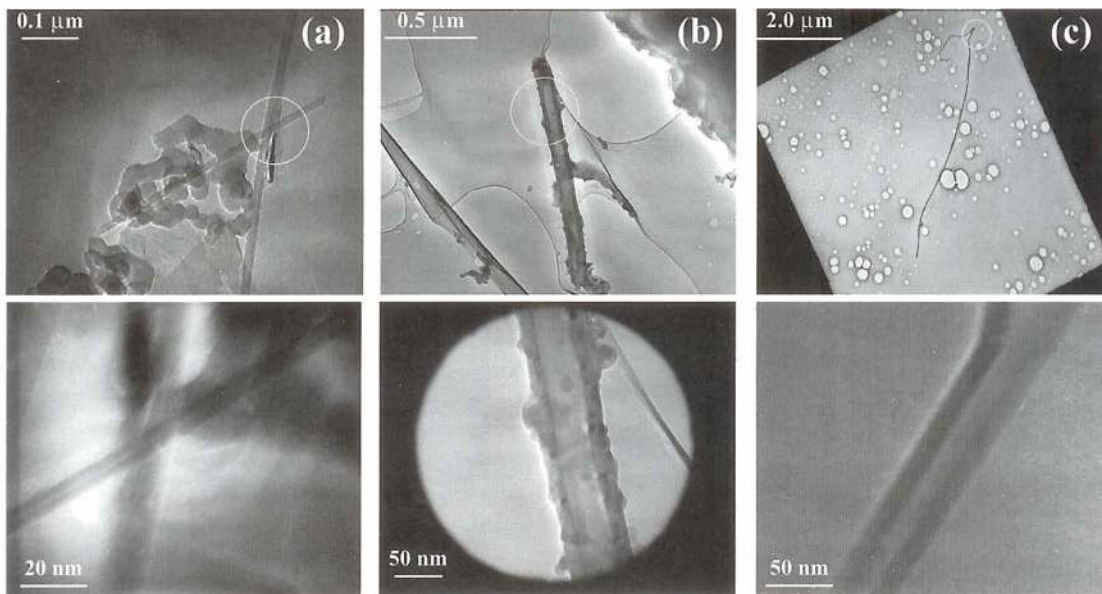


Fig. 2. TEM images of the fibrous nanostructures from the (a) 1-hour, (b) 3-hour and (c) 5-hour samples indicate approximately micron lengths and hollow core structures.

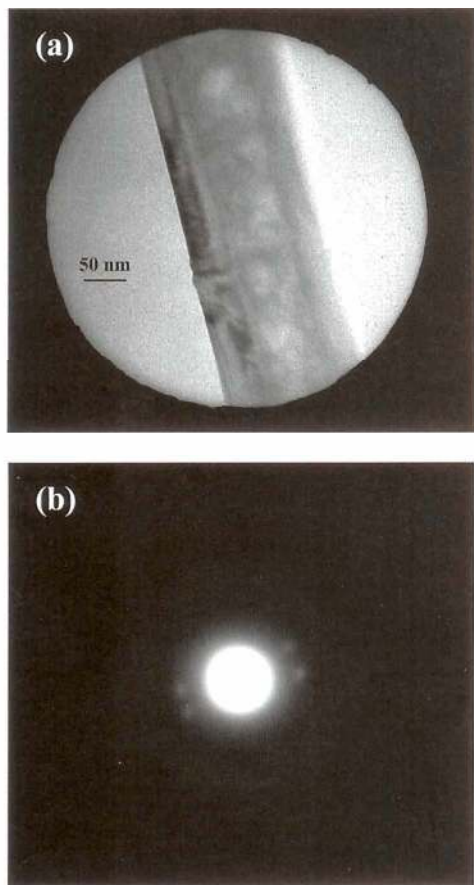


Fig. 3. (a) Bright field image with SAD aperture overlay and (b) rotationally correct SAD diffraction pattern showing spot splitting indicative of carbon nanotubes. Amorphous rings may be from either the tube surface structure or from the carbon support film.

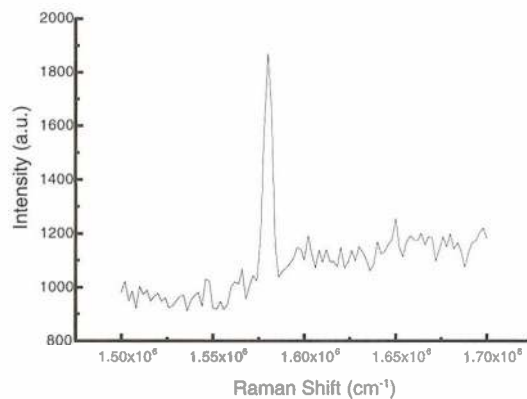


Fig. 4. Micro Raman and Surface Enhanced Micro Raman Spectroscopy (SERS) from the 5-hour sample indicate the formation of well graphitized carbon nanostructures by relatively sharp peaks with FWHM about 8–10 cm^{-1} at 1580 cm^{-1} .

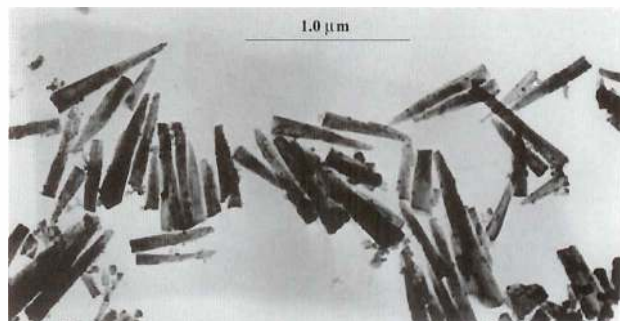


Fig. 5. TEM images from the 1-hour, 3-hour and 5-hour samples indicate that tapered silicon nanostructures were etched perpendicular to the surface. The above image is from the 5-hour sample.

RESEARCH ARTICLE

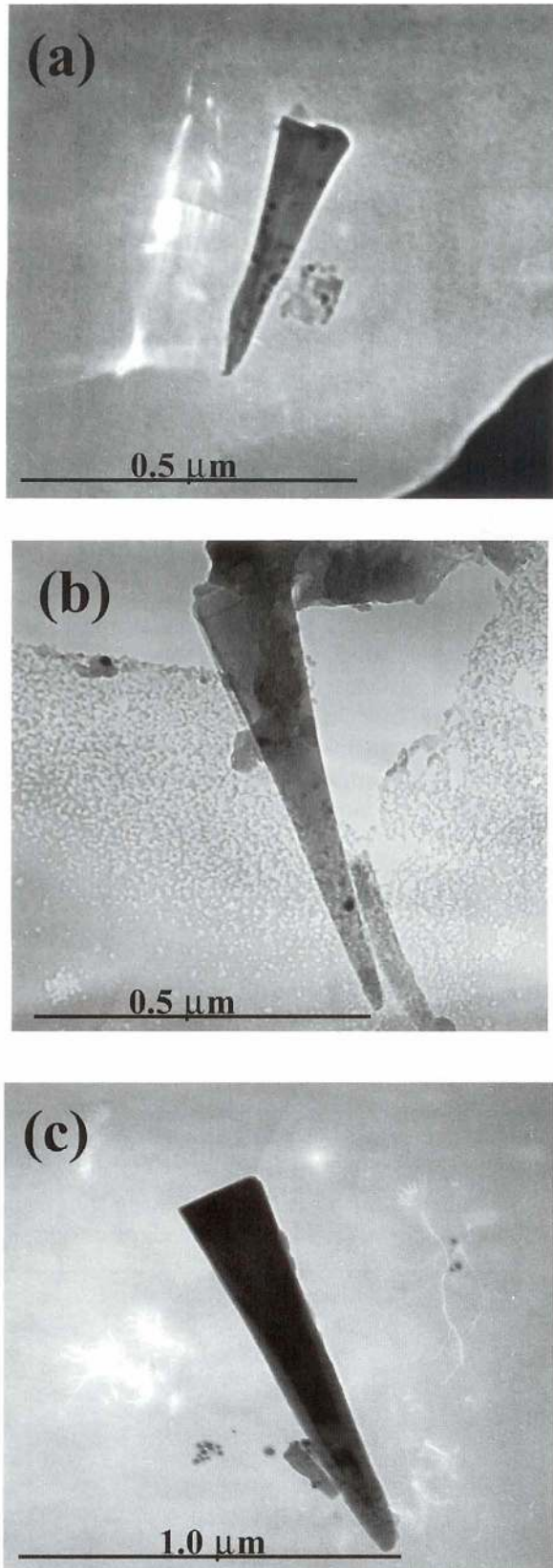


Fig. 6. TEM images indicate that the lengths of the tapered nanostructures varied progressively as a function of time: (a) 1-hour, (b) 3-hour, and (c) 5-hour samples.

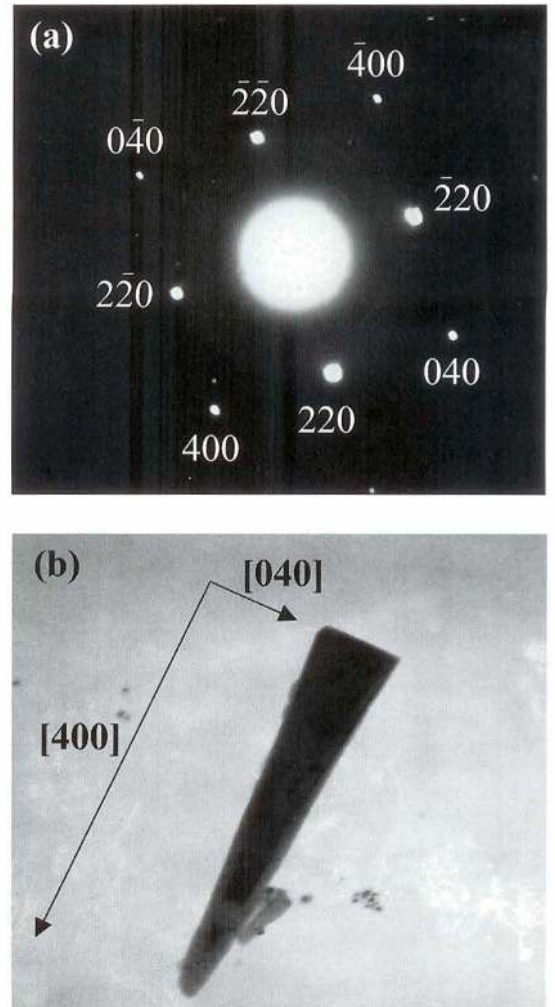


Fig. 7. SAD diffraction images from the tapered nanostructures show patterns indicative of single crystal silicon with the [100] orientation along the long axis.

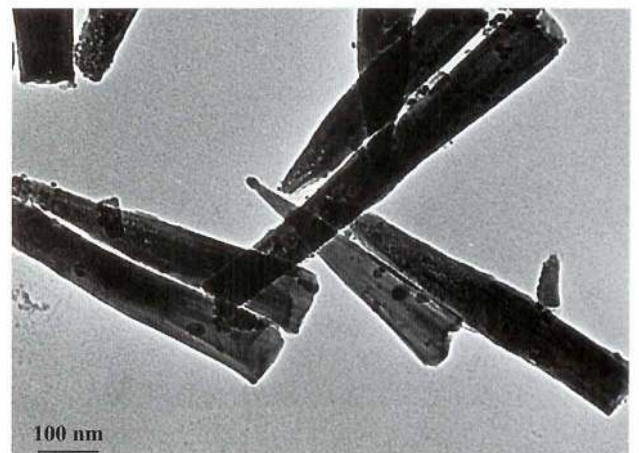


Fig. 8. Dark contrast dots at the tips and along the sides of the tapered silicon nanowires were shown to be iron.

dots were subsequently shown by HRTEM to be nanocrystalline iron.

3.3. High Resolution Transmission Electron Microscopy and EDS Results

HRTEM was used to assess details of the silicon, carbon and iron nanostructures. Two size scales of fibrous carbon nanostructures were observed. Based on inner and outer diameters, these were identified as multi-walled carbon nanotubes and vapor-grown carbon nanofibers, as shown in Fig. 9. Background from the carbon holey film limited further resolution of the wall structures. The dark contrast dots were shown by HRTEM to be crystalline with well-defined atomic spacings consistent with bcc iron. EDS spectra provided further confirmation that these dark contrast features contained predominantly iron. The HRTEM and EDS results are shown in Fig. 10 (a)–(d). Iron nanodots were sometimes observed at the tips of the carbon nanostructures, as well as at the tips of the tapered silicon nanowires, as shown in the Figure 9 insert.

Details of a heterojunction between a tapered silicon nanowire tip and a multi-walled carbon nanotube are shown in Fig. 11 (a)–(c). The heterojunction appears to be

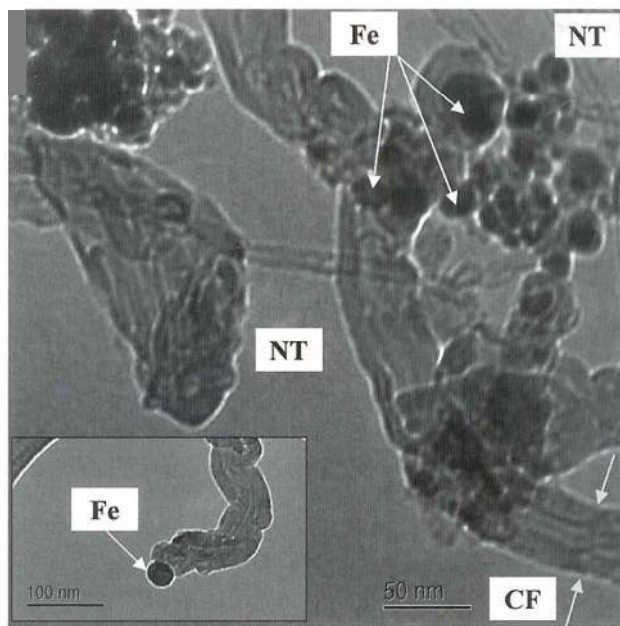


Fig. 9. HRTEM images indicate multi-wall carbon nanotubes (NT) and vapor grown carbon nanofibers (CF). Iron (Fe) dots were sometimes observed at the tips of the carbon nanostructures as shown in the lower left corner insert.

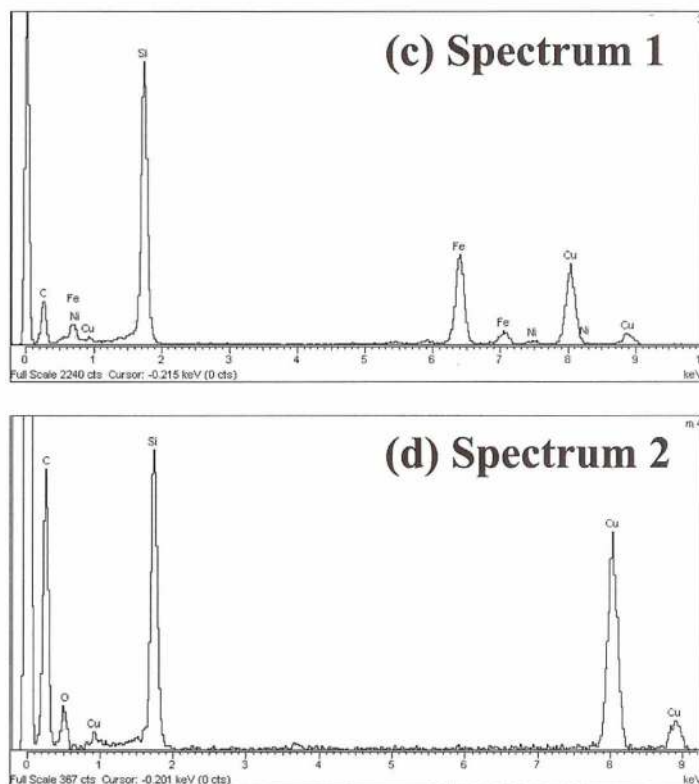
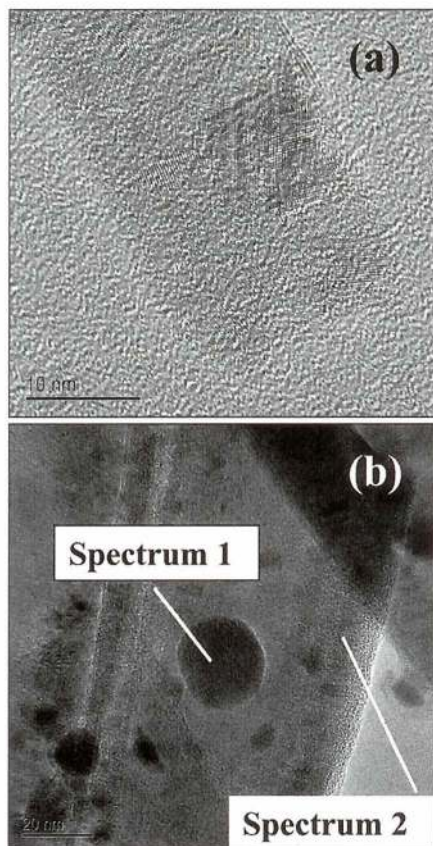


Fig. 10. (a) The dark contrast dots showed atomic spacings consistent with nanocrystalline iron (scale bar, 10 nm). (b) EDS spectra (scale bar, 20 nm) were used to further confirm the identification of the (c) iron nanodots (Spectrum 1) on the (d) silicon nanowires (Spectrum 2).

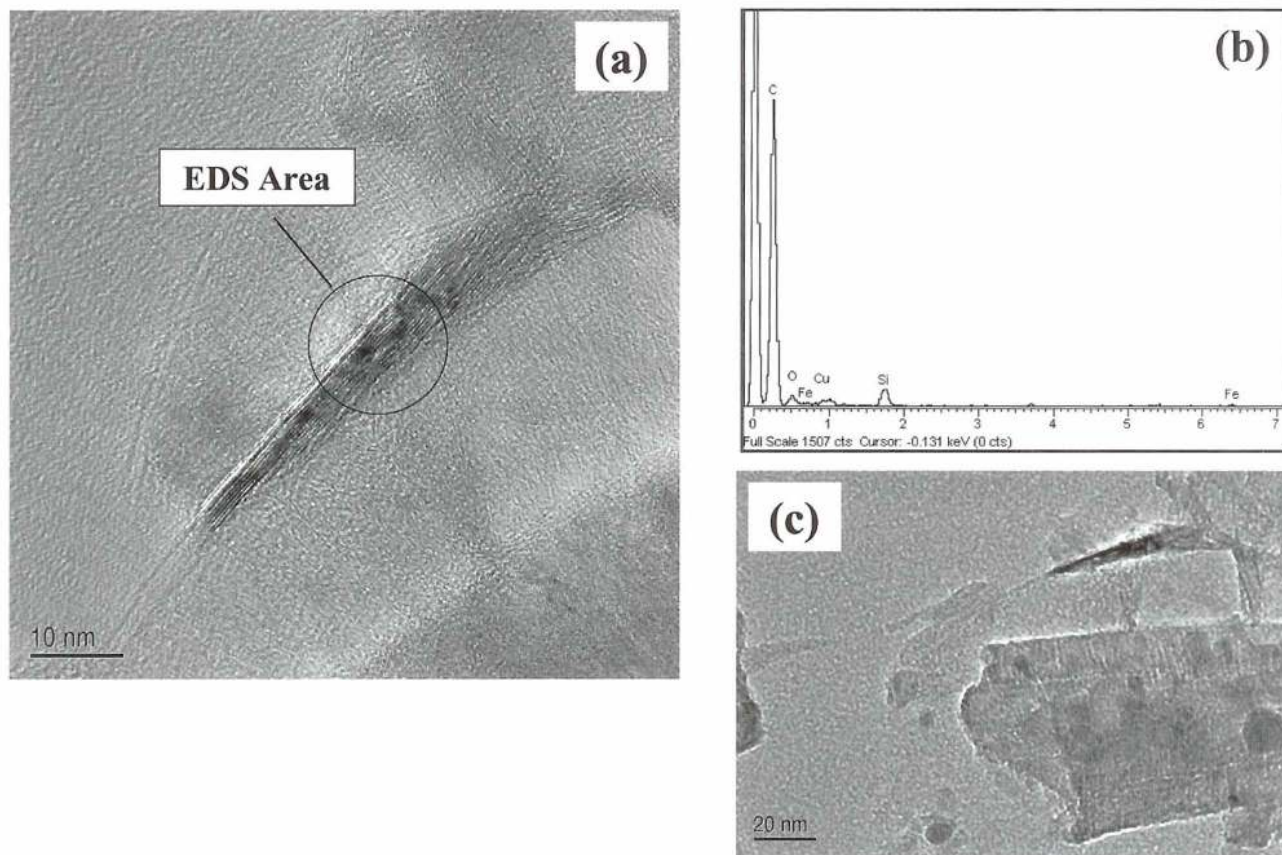


Fig. 11. (a) HRTEM image of a heterojunction between a MWCNT and a tapered silicon nanowire tip. (b) EDS was used to support the silicon identification (c) Lower magnification view of the MWCNT-silicon nanowire heterojunction.

about 4–6 nm wide. An EDS spectrum, shown in Fig. 11 (b), provided further support for the identification of distinct silicon and carbon component parts.

Two types of nanostructures were observed in the plane of, and perpendicular to, the sample surfaces for 1 hour 0 minutes, 3 hours 10 minutes and 5 hours 23 minutes reactor times. One was fibrous and micron-scale in length for all reactor times. The other was tapered, solid and with an aspect ratio which changed as a function of reactor time. Analysis by TEM/SAD, HRTEM/EDS and micro-Raman/SERS indicated that the material compositions of these nanostructures were, respectively, carbon and silicon.

The carbon nanostructures were shown by TEM and HRTEM to be multi-walled carbon nanotubes and hollow core vapor-grown carbon nanofibers. The iron catalyst layer was shown by TEM and HRTEM to be broken up into 10s of nanometer-sized droplets by the action of the plasma. Iron dots of 5–20 nm diameter were observed at the tips and along the sides of most of the tapered silicon nanowires. They were also observed at the ends of some of the carbon nanotubes and nanofibers. The observed multi-walled carbon nanotubes and carbon nanofibers

would be consistent with growth via a Liquid-Metal-Solid growth mechanism in the presence of the iron catalyst droplets.

The silicon nanowires were shown by TEM and SAD to be solid tapered nano-wires, with the [100] orientation in the sample normal direction, and with progressive length variations as a function of reactor time. This result is consistent with formation by an etching mechanism of the (100) silicon substrate. Similar etchings of silicon^{11, 12} and other semiconductor materials^{13, 14} have been observed in argon-methane plasmas. However, in our experiments, the etching of the silicon nanostructures was simultaneously accompanied by LMS-mechanism growth of the carbon nanostructures. As the iron catalyst layer was broken up into 10s of nanometer-sized islands by the action of the plasma, it may have served as a nano-mask for the etching of silicon, as well as the LMS nucleation site for the growth of the multi-walled carbon nanotubes.

SEM images indicated that a nano-heterostructure junction was formed between the carbon nanostructures and the silicon nanowires at the pointed tips of the silicon. The formation of such junctions was observed for all three reactor times. The sample preparation method used in the present

analysis reduced the probability of finding an intact heterojunction, but one intact specimen was located and analyzed by HRTEM. The multi-walled carbon nanotube-silicon nanowire heterojunction appears to be about 4–6 nm wide, which is a truly nanoscale heterojunction. Further experiments are needed to determine how many junctions had a similar structure, and if this type of connection is found within the macroscopic junctions observed by SEM.

We conclude that conditions for simultaneous LMS growth of multi-walled carbon nanotubes and etching of high aspect ratio silicon nanowires can be achieved in an inductively coupled plasma reactor system. ICP reactors are state-of-the-art semiconductor fabrication industry tools for large-scale silicon etching, due to high radial uniformity and low pressure/low temperature operating characteristics. Our results indicate that the incorporation of nano-materials produced by an LMS growth mechanism within a growth/etching fabrication cycle may also be possible. This may, in turn, lead to practical large-scale manufacturing of nano-components of multiple materials, using an existing reactor tool for both conventional silicon and new nano-electronic materials.

4. SUMMARY

We report the formation of carbon nanotube and silicon heterostructures in an inductively coupled plasma system by a simultaneous growth/etching mechanism. This is an alternative method for the formation of a hetero carbon nanotube-silicon nanowire interface that can provide increased processing flexibility.

Acknowledgments: S. P. S. acknowledges the Harriet G. Jenkins UNCF-NASA Fellowship Program. Laser-ablated iron catalyst depositions were provided by B. Qi/R. Gilgen-

bach. Helpful discussions with M. Kushner, F. Terry and R. Gilgenbach are gratefully acknowledged.

References and Notes

1. M. S. Gudiksen, L. J. Lauhon, J. Wang, D. C. Smith, and C. M. Lieber, *Nature* 415, 617 (2002); C. M. Lieber, *Nano Lett.* 2, 81 (2002); J. Hu, M. Ouyang, P. Yang, and C. M. Lieber, *Nature* 399, 48 (1999).
2. Y. Wu, R. Fen, and P. Yang, *Nano Lett.* 2, 83 (2002).
3. M. T. Bjork, B. J. Ohlsson, T. Sass, A. I. Persson, C. Thelander, M. H. Magnusson, K. Deppert, L. R. Wallenberg, and L. Samuelson, *Appl. Phys. Lett.* 80, 1058 (2002); M. T. Bjork, B. J. Ohlsson, T. Sass, A. I. Persson, C. Thelander, M. H. Magnusson, K. Deppert, L. R. Wallenberg, and L. Samuelson, *Nano Lett.* 2, 87 (2002).
4. Y. F. Zhang, Y. H. Tang, Y. Zhang, C. S. Lee, I. Bello, and S. T. Lee, *Chem. Phys. Lett.* 330, 48 (2000).
5. G. A. Hebner, *J. Appl. Phys.* 80, 2624 (1996).
6. P. Hargis Jr., K. Greenberg, P. Miller, J. Gerado, J. Torczynski, M. Riley, G. Hebner, J. Roberts, J. Olthoff, J. Whetstone, R. Van Brunt, M. Sobolewski, H. Anderson, M. Splichal, J. Mock, P. Bletzinger, A. Butterbaugh, M. Brake, M. Passow, J. Pender, A. Lujan, M. Elta, D. Graves, H. Sawin, M. Kushner, J. Verdeyen, R. Horwath, and T. Turner, *Rev. Sci. Instr.* 65, 140 (1994).
7. C. J. Collard, Ph.D. Thesis, The University of Michigan, (2002).
8. B. Qi, R. M. Gilgenbach, Y. Y. Lau, M. D. Johnston, J. Lian, L. M. Wang, G. L. Doll, and A. Lazarides, *Appl. Phys. Lett.* 78, 3785 (2001); B. Qi, Y. Y. Lau, R. M. Gilgenbach, *Appl. Phys. Lett.* 78, 706 (2001).
9. P. Corio, S. D. M. Brown, A. Marucci, M. A. Pimenta, K. Kneipp, G. Dresselhaus, and M. S. Dresselhaus, *Phys. Rev. B* 61, 13202 (2000).
10. L. C. Qin, T. Ichihashi, and S. Iijima, *Ultramicroscopy* 67, 181 (1996).
11. G. S. Oerhleim, J. F. Rembetski, and E. H. Payne, *J. Vac. Sci. Technol. B* 8, 1199 (1990).
12. E. I. Givargizov, A. N. Stepanova, L. N. Obolenskaya, E. S. Mashkova, V. A. Molchanov, M. E. Givargizov, and I. W. Rangelow, *Ultramicroscopy* 82, 57 (2000).
13. P. S. Nam, L. M. Ferreira, T. Y. Lee, and K. N. Tu, *J. Vac. Sci. Technol. B* 18, 2780 (2000).
14. J. E. Parmeter, R. J. Shul, A. J. Howard, and P. A. Miller, *J. Vac. Sci. Technol. B* 18, 3563 (1996).

Received: 24 December 2003. Revised/Accepted: 6 January 2004.